

ELECTRONIC SUPPORTING INFORMATION

Probing framework-guest interactions in phenylene-bridged periodic mesoporous organosilica using spin-probe EPR

Feng Lin, Xiangyan Meng, Myrjam Mertens, Pegie Cool, and Sabine Van Doorslaer

1. TGA analyses of phenylene-bridged PMO materials

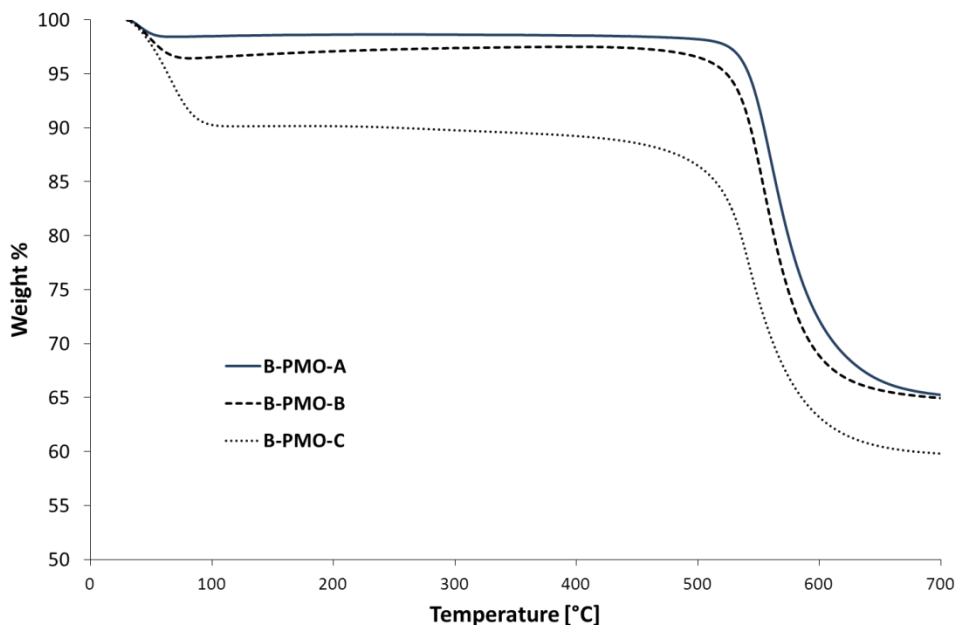


Figure S1: TGA curves of the three types phenylene-bridged PMO materials under study.

The TGA curves in Figure S1 complement the DTG analysis shown in Figure 3, main text.

2. Additional analysis of FT-IR spectra of phenylene-bridged PMO materials

The FT-IR spectra of the three types phenylene-bridged PMOs (template-free) are shown in the range of 500 cm^{-1} - 4000 cm^{-1} (Figure S2). It has already been shown in the main text that, compared with B-PMO-A and B-PMO-B, B-PMO-C, contains much more surface water and silanols. However, it is interesting to notice another clear difference between the spectra of B-PMO-A and B-PMO-B (or B-PMO-C). Both the FT-IR spectra of B-PMO-B and B-PMO-C, containing the amorphous walls, exhibit a broad peak centered at 640 cm^{-1} (indicated with “?” in Figure S2), while this peak is absent in the FT-IR spectra of B-PMO-A with the crystal-like pore wall. It seems that this peak is related to the molecular-scale arrangement of the aromatic rings in the wall of the phenylene-bridged PMOs. There are three possibilities of the assignment of this peak: (i) Si-C stretching vibrations, (ii) Si-O-H in-plane and out-of-plane bending, and (iii)

aromatic C-H bending. An experimental and theoretical Raman and IR analysis of phenylene-bridged PMOs by Hoffmann et al.¹ gives evidence that this band is not caused by Si-C modes. Since the band at 640 cm^{-1} can still be observed in the FT-IR spectra of the dehydrated B-PMO-B and B-PMO-C (not shown), it means that the peak cannot be assigned to the Si-O-H bending. Thus, this band is most likely due to the C-H deformation modes. Interestingly, the band is not observed in the FT-IR spectra of B-PMO-A. It is known that the crystal-like pore wall of B-PMO-A, observed as molecular periodicity, is due to the π - π stacking of the phenylene bridging units. This π - π stacking of the phenylene rings may greatly limit the aromatic C-H deformation modes, whereas in B-PMO-B and B-PMO-C, which lack the molecular periodicity, the aromatic C-H deformation modes can be clearly observed. This suggests that FT-IR can be used to distinguish the molecular-scale arrangement of the aromatic rings in the wall of the phenylene-bridged PMO materials. Nevertheless, it is still challenging to point out a definite assignment of this band.

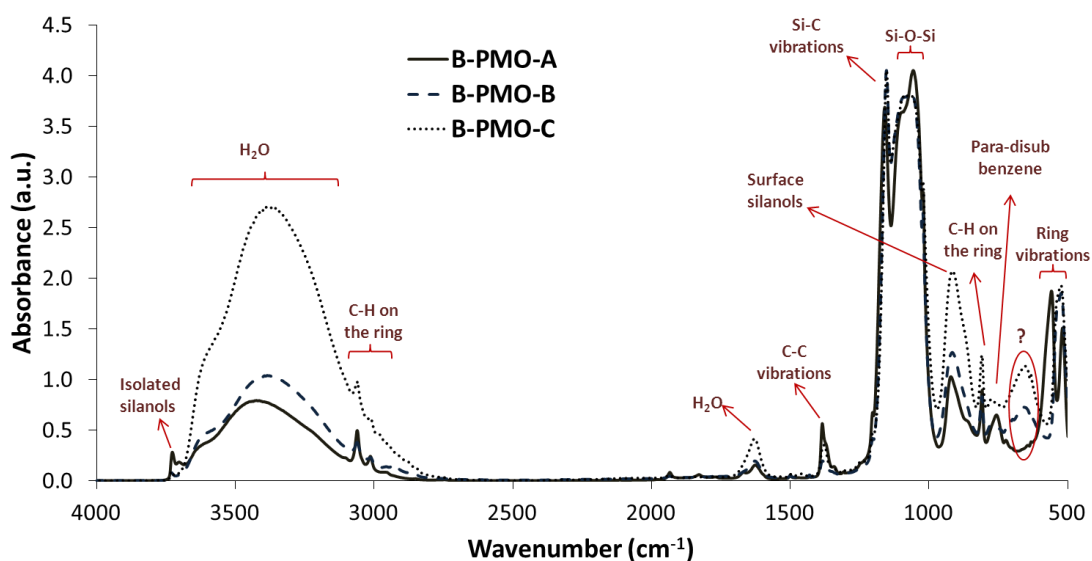


Figure S2: Detailed assignment of the FT-IR spectra of the template-free phenylene-bridged PMO materials under study

3. EPR spectra of 3-CP in phenylene-bridged PMOs: spin-probe mobility analysis

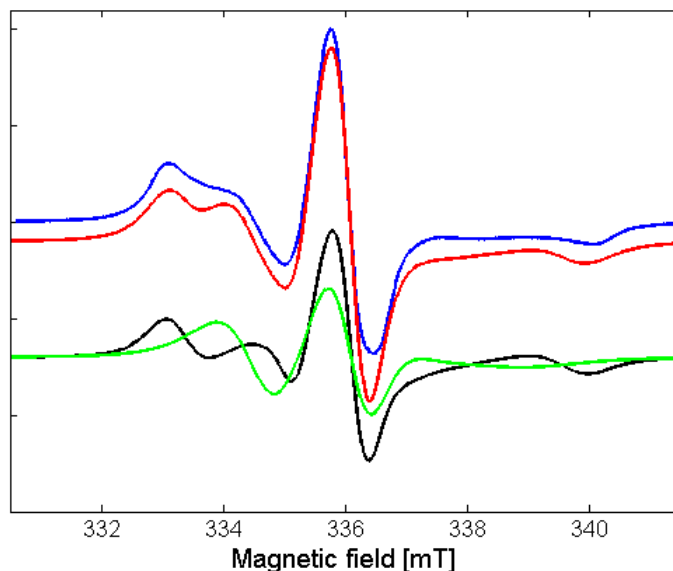


Figure S3. Blue: Experimental X-band CW-EPR spectrum of 3-CP adsorbed on dehydrated **B-PMO-C** measured at room temperature. Red: simulation with the experimental parameters from Table S1. Green: contribution of fast tumbling 3-CP (F1), Black: contribution of slow tumbling 3-CP (S1).

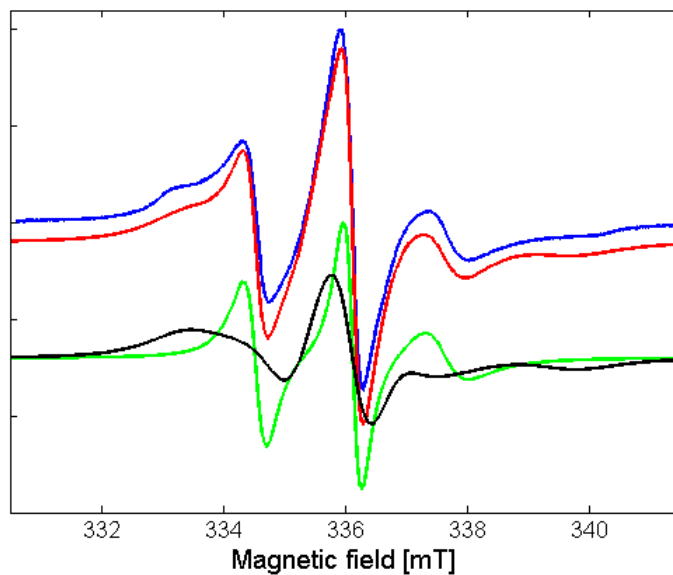


Figure S4. Blue: Experimental X-band CW-EPR spectrum of 3-CP adsorbed on dehydrated **B-PMO-B** measured at room temperature. Red: simulation with the experimental parameters from Table S1. Green: contribution of fast tumbling 3-CP (F2), Black: contribution of slow tumbling 3-CP (S2).

Table S1. Simulation parameters used to simulate the spectra represented in Figures S3 and S4. D_x , D_y , D_z are the principal components of the rotational diffusion tensor. $D^r = \sqrt[3]{D_x D_y D_z}$ is the overall rotational diffusion parameter and τ_d the related rotational correlation time ($\tau_d = \frac{1}{6D^r}$). All simulations were done taking $A=[13.7 \ 13.5 \ 111]$ MHz and $g=[2.0088 \ 2.0065 \ 2.0028]$. All simulations were done using the EasySpin program².

	D_x (x10 ⁷ /s)	D_y (x10 ⁷ /s)	D_z (x10 ⁷ /s)	D^r (x10 ⁷ /s)	τ_d (ns)	%	fraction
3-CP on	9.42	10.65	13.52	5.13	3.24	19	F2
B-PMO-B	3.00	4.61	2.56	3.28	5.08	81	S2
3-CP on	13.24	0.77	6.52	4.05	4.10	42	F1
B-PMO-C	2.07	1.65	3.82	2.36	7.05	58	S1

As has been shown extensively (e.g. reference 38 of the main text), a correct determination of the motional parameters of nitroxide labels from EPR can only be achieved when experiments are performed at different microwave frequencies. However, a number of qualitative parameters can already be obtained from the analysis of the spectra at one microwave frequency, as is demonstrated here for the case of 3-CP adsorbed on dehydrated B-PMO-C and B-PMO-B (Figures S3 and S4). First of all, none of the X-band EPR spectra can be simulated assuming a single population of spin probes with a specific motional behavior. As can be seen from Figs. S3 and S4, the main features of the spectra can be reproduced assuming two motional fractions, hereafter called a fast (F1 or F2) and a slow (S1 or S2) phase (Table S1, Figs. S3 and S4). It is however clear that the EPR spectra are still not perfectly reproduced in this way, implying that additional smaller motional fractions (phases) will be present. The parameters mentioned in Table S1 should therefore only be interpreted in a qualitative manner and only trends should be evaluated. We notice that τ_d (F2) < τ_d (F1) and τ_d (S2) < τ_d (S1), so the motion of the spin probe seems to be more reduced in the case of the B-PMO-C. A similar conclusion also follows from analysis of the two low-field peaks marked in Figure 4 (main text) with the solid and dashed arrow. Inspection of Figures S3 and S4 indeed shows that these two signals can be used as markers for the slow and fast motion phases. This is also explained in the main text.

4. Evaluation of the dipolar interaction between the spin probes adsorbed on the surface of B-PMOs

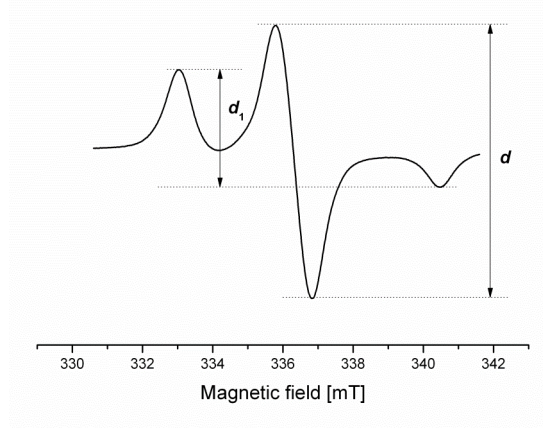


Figure S5: X-band CW-EPR spectrum of 3-CP adsorbed on B-PMO-A measured at 10 K. The peak intensities (d and d_1) are defined as shown by the arrows.

Table S2 shows the different d_1/d values obtained for the different low-temperature EPR spectra of the spin probes adsorbed on the three types of B-PMO materials under study (see Figure S5 for an example of such a spectrum). The d_1/d value is dependent on the inter-spin-probe distance: the higher the value, the closer the spin probes are on average in space. For all the spin probes, we find the highest values for incorporation in B-PMO-A, agreeing with the room temperature observations. In order to determine the exact distances from the d_1/d values, one needs good reference systems with similar geometrical distribution of the spin probes (on surface of pores), similar polarity of the environment (which influences the hyperfine value, which in turn influences the d_1/d values) and with known distances. Since this is not available, we here limit ourselves to the qualitative analysis. However, it should be noted that since changes in the d_1/d values are observed between the different systems, we are in the range where the dipolar interaction influences the CW-EPR spectra, *i.e.* we have inter-spin distances below 3 nm. This is smaller than the average inter-spin distance, x_{rand} , determined assuming randomly adsorbed molecules using the random distribution law (ref. 43, main text)

$$x_{rand} = \Gamma\left(\frac{3}{2}\right) \sqrt{\frac{S}{\pi c}}$$

with Γ the gamma function, S the surface area reported in Table 1, c is the number of spins/g from the spin concentration reported in Table 2. The corresponding x_{rand} values can be found in Table S3 and exceed 7.3 nm. From this, we can conclude that the spin probes are not equally distributed over the material and cannot fully penetrate the material.

Table S2. d_1/d values for 3-CP, 4-HTB, TEMPO adsorbed on different phenylene-bridged PMOs

Spin probe	Sample	d_1/d
3-CP	B-PMO-A	0.43
	B-PMO-B	0.39
	B-PMO-C	0.37
4-HTB	B-PMO-A	0.52
	B-PMO-B	0.48
	B-PMO-C	0.44
TEMPO	B-PMO-A	0.46
	B-PMO-B	0.41
	B-PMO-C	0.41

Table S3. Average inter-spin distance x_{rand} in nm determined assuming randomly adsorbed molecules using the experimental spin concentrations and surface area (see above).

	B-PMO-A	B-PMO-B	B-PMO-C
3-CP	9.6	8.8	7.3
4-HTB	29.7	14.7	13.3
TEMPO	15.3	13.5	10.2

5. Comparison of the EPR spectra before and after rehydration of the PMO materials

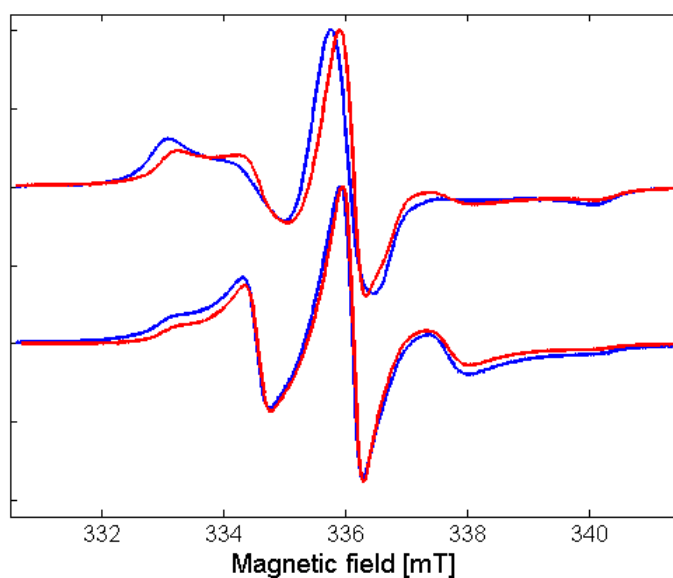


Figure S6. Comparison between the X-band CW-EPR spectra before (blue) and after (red) dehydration. (top) 3-CP in B-PMO-C and (bottom) 3-CP in B-PMO-B. The spectra are shown normalized to the central line in order to allow facile comparison.

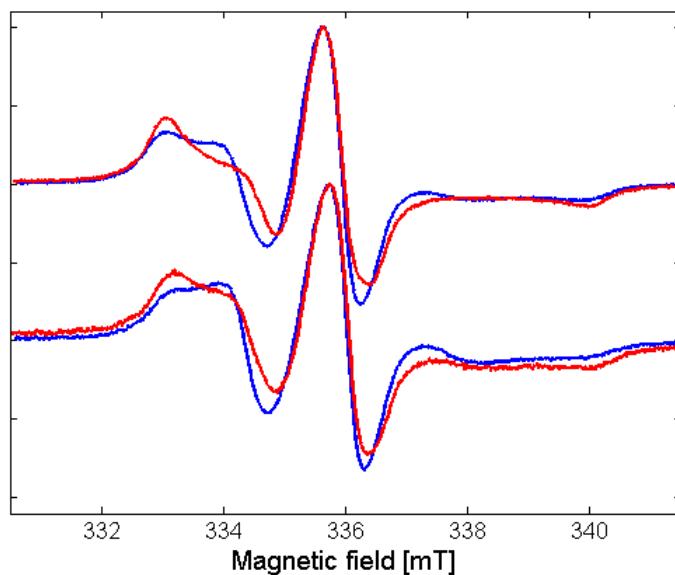


Figure S7. Comparison between the X-band CW-EPR spectra before (blue) and after (red) dehydration. (top) 4-HTB in B-PMO-C and (bottom) 4-HTB in B-PMO-B. The spectra are shown normalized to the central line in order to allow facile comparison.

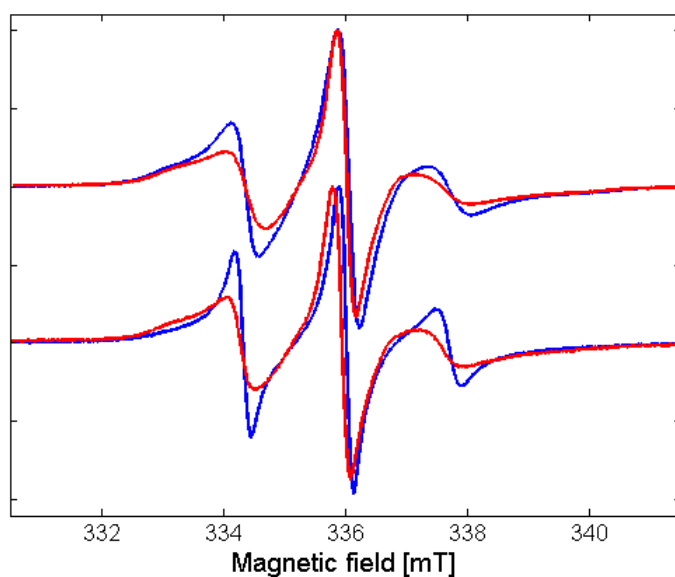


Figure S8. Comparison between the X-band CW-EPR spectra before (blue) and after (red) dehydration. (top) TEMPO in B-PMO-C and (bottom) TEMPO in B-PMO-B. The spectra are shown normalized to the central line in order to allow facile comparison.

Figures S6 to S8 show a pair-wise overlay of the CW-EPR spectra for all spin probes in B-PMO-B and B-PMO-C before and after rehydration. This representation allows a facile evaluation of the spectral changes. From Figures S7 and S8, it is immediately clear that dehydration causes in both PMOs a slower motion of

the spin probes 4-HTB and TEMPO (clearly visible from the change in the two low-field marker signals as explained in section 3 and in the main text). The EPR spectrum of 3-CP in B-PMO-B remains quasi unchanged after dehydration, while a small spectral change indicative of a faster motion of 3-CP is observed for B-PMO-C (Figure S6). In all cases, the motional behavior remains complex.

6. Details of synthesis of ethylene-bridged PMO materials

The synthesis method reported by Inagaki *et al.*³ was employed to prepare the ethylene-bridged PMO materials. In a typical synthesis procedure, C₁₆TMACl (2.13 g) was added under vigorous stirring to a solution of 1.09 g of NaOH in 72.60 g of water. After complete dissolution of the surfactant, 3ml of BTME was added. The final reactant molar composition was: 1.0 BTME : 0.57 C₁₆TMACl : 2.36 NaOH : 353 H₂O. After the samples were mixed as described above, the solution was aged under stirring for 24 h at room temperature and then heated at 95 °C for 20-24 h without stirring. Surfactant template removal was accomplished by two solvent extraction cycles with ethanol containing HCl at 333 K.

7. CW-EPR of spin-probe adsorption on ethylene-bridged PMO compared to B-PMO-B

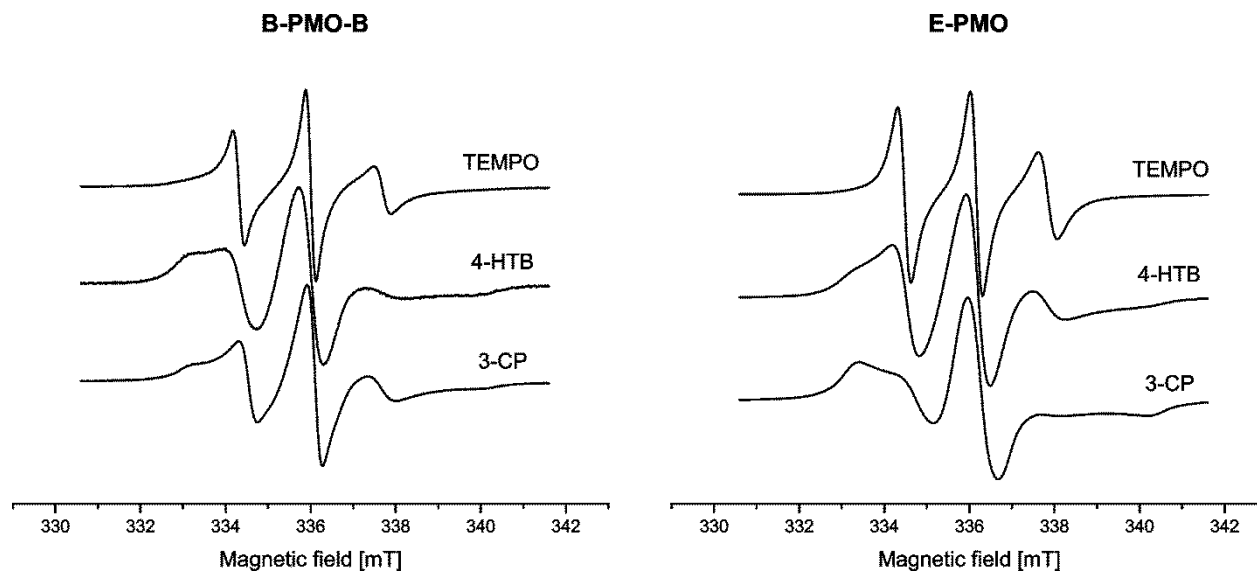


Figure S9: Room-temperature CW-EPR spectra of 3-CP, 4-HTB and TEMPO adsorbed on dehydrated B-PMO-B and ethylene-bridged PMO (E-PMO) materials. The same procedure for dehydration and spin-probe adsorption was used for the two materials. The mobility of 3-CP is lower in E-PMO than in B-PMO-B (as can be derived, amongst others, from the higher signal intensity of the feature at lowest field). For the other two spin probes, the mobility is highest in the E-PMO.

References

- 1 F. Hoffmann, M. Güngerich, P. J. Klar, and M. Fröba. *J. Phys. Chem. C*, 2007, **111**, 5648
- 2 S. Stoll, A. Schweiger, *J. Magn. Reson.*, 178, 42 (2006).
- 3 S. Inagaki, S. Guan, Y. Fukushima, T. Ohsuna, and O. Terasaki. *J. Am. Chem. Soc.*, 1999, **121**, 9611.